Effects of Time Delay Between Unipolar Pulses in High Frequency Nano-Electrochemotherapy

Vitalij Novickij, Austėja Balevičiūtė, Veronika Malyško, Augustinas Želvys, Eivina Radzevičiūtė, Bor Kos, Auksė Zinkevičienė, Damijan Miklavčič, Jurij Novickij, and Irutė Girkontaitė

***Abstract*—*Objective:* this work focuses on bleomycin electrochemotherapy using new modality of high repetition frequency unipolar nanosecond pulses. *Methods:* As a tumor model, Lewis lung carcinoma (LLC1) cell line in C57BL mice (n = 42) was used. Electrochemotherapy was performed with intertumoral injection of bleomycin (50 μL of 1500 IU solution) followed by nanosecond and microsecond range electrical pulse delivery via parallel plate electrodes. The 3.5 kV/cm pulses of 200 and 700 ns were delivered in a burst of 200 at frequencies of 1 kHz and 1 MHz. For comparison of treatment efficiency, a standard 1.3 kV/cm x 100 μs x 8 protocol was used. *Results:* It was shown that it is possible to manipulate the efficacy of unipolar sub-microsecond electrochemotherapy solely by the time delay between the pulses. *Significance:* the results suggest that the sub-microsecond range pulses can be as effective as the protocols in European Standard Operating Procedures on Electrochemotherapy (ESOPE) using 100 μs pulses.**

***Index Terms*—Sub-microsecond electroporation, in vivo, mice, LLC1, high frequency pulses.**

I. Introduction

ELECTROPORATION is a phenomenon of increased permeability of the cell membrane, which is triggered by high intensity pulsed electric fields (PEF). Depending on the parameters of PEF the cellular response, pore density/size and electrotransfer efficiency can be manipulated [1], [2]. Therefore, the research of optimal pulse parameters and protocols [3], [4], the susceptibility patterns of various cancers [5] and the technological development of electroporation platforms [6], [7] is constantly performed. In case of high intensity pulses, electroporation can be used as a non-thermal tissue ablation method, also known as irreversible electroporation (IRE) [8], [9]. In such a case the amplitude of electric field is significantly higher than the threshold for cell membrane permeabilization and the number of pulses in a burst exceeds tens or even hundreds [10], [11]. Combination of electroporation with chemotherapy (i.e., with bleomycin or cisplatin) resulted in a well-established electrochemotherapy methodology [12]. The European Standard Operating Procedures on Electrochemotherapy (ESOPE) involve application of 100 μs x 8 pulses delivered with predefined 1 Hz or a few kHz repetition frequency in combination with cisplatin or bleomycin [13]. Nevertheless, the field is moving towards shorter pulses due to better control of the energy of the burst, which is due significantly higher number of pulses, shorter rise and fall times and higher electric field amplitudes used in nanosecond parametric protocols when compared to ESOPE procedures. Potentially it offers a more uniform tumor exposure, better control of thermal effects and the capabilities to trigger additional cellular mechanisms in the nanosecond pulse range [14]–[16]. However, the number of reports on nanosecond range electrochemotherapy is limited. Typically, the nanosecond methodology was applied in IRE context [17], while nano-electrochemotherapy works started to appear only recently [18]–[21].

Moreover, pulse duration and amplitude of PEF are not the only parameters governing the treatment during nanosecond electroporation. A few years ago, a new time delay-dependent unipolar electroporation phenomenon was confirmed [22], [23] and it was shown that high frequency (>100 kHz) pulse bursts induce higher permeabilization compared to the PEF bursts of the same energy but delivered at lower frequency. The phenomenon was verified both *in vitro* and *in silico* [24]. We have shown that the number of permeabilized cells can be doubled solely by decrease of the delay between the pulses without any changes in the total energy of the burst [25]. By means of generating high-frequency pulse sequences (MHz range), it is possible to achieve a threshold repetition frequency when the discharging (transmembrane potential (TMP) relaxation) time of the membrane is higher than the time delay between the pulses, and thus the TMP starts to accumulate throughout the burst [22], [25], [26]. The time delay-dependent unipolar electroporation phenomenon was not yet confirmed *in vivo*.

In this work we provide the first *in vivo* data on sub-microsecond unipolar electrochemotherapy using MHz repetition pulse sequences to exploit the phenomenon of TMP accumulation. The results are useful for development of new treatment efficiency-wise ESOPE-equivalent, but nanosecond protocols supporting the transaction of electrochemotherapy towards shorter pulse range.

Manuscript received May 11, 2021; revised September 24, 2021; accepted November 16, 2021. Date of publication November 19, 2021; date of current version April 21, 2022. This work was supported in part by the Research Council of Lithuania, Grant S-MIP-19-22. *(Corresponding author: Vitalij Novickij.)*

Vitalij Novickij, Veronika Malyško, and Jurij Novickij are with the Vilnius Gediminas Technical University, Lithuania.

Austėja Balevičiūtė, Augustinas Želvys, Eivina Radzevičiūtė, Auksė Zinkevičienė, and Irutė Girkontaitė are with the State Research Institute Centre for Innovative Medicine, Lithuania.

Bor Kos and Damijan Miklavčič are with the University of Ljubljana, Slovenia.

Digital Object Identifier 10.1109/TBME.2021.3129176

TABLE I
TARGET ELECTROPORATION PROTOCOLS

Protocol	Pulse parameters	Energy (J)*
nsPEF1	3.5 kV/cm x 200 ns x 200, 1 kHz	~0.5
nsPEF2	3.5 kV/cm x 200 ns x 200, 1 MHz	~0.5
nsPEF3	3.5 kV/cm x 700 ns x 200, 1 kHz	~1.6
nsPEF4	3.5 kV/cm x 700 ns x 200, 1 MHz	~1.6
µsPEF	1.3 kV/cm x 100 µs x 8, 1 Hz	~0.9

*Transients are not considered.

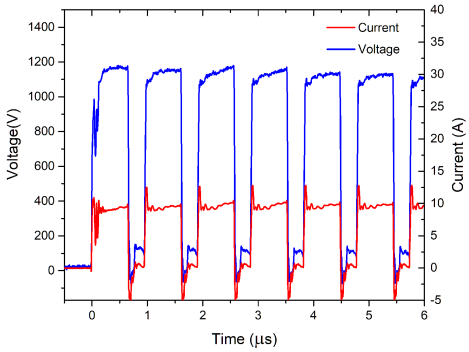

Fig. 1. Voltage and current waveforms on a superficial LLC tumor. Measured using DPO4034 oscilloscope (Tektronix, Beaverton, USA) and P4250 probe (Cleqee, Shenzhen, China), post-processed using OriginPro Software (OriginLab, Northampton, USA).

II. MATERIALS AND METHODS

A. Electroporation Setup

Up to 3 kV, 100 ns – 1 ms square wave high voltage and high frequency pulse generator was used for electroporation [27]. The generator is capable of generating bursts of pulses with predefined pulse repetition rate in the 1 Hz – 1 MHz range (software limited; hardware limited at 3+ MHz). For *in vitro* experiments, commercially available electroporation cuvette with 1 mm gap aluminum electrodes (Biorad, Hercules, USA) was used as an exposure setup to generate up to 3.5 kV/cm electric field. The duration of the pulses was 200, 700 ns and 100 μs. Sub-microsecond pulses were delivered in bursts of 200 with 1 kHz or 1 MHz repetition frequency. The 100 μs pulses were delivered in a sequence of 8 with a 1 Hz repetition frequency according to ESOPE protocol and were used as a reference. For *in vivo* experiments, the same pulse protocols were delivered using two parallel plates steel electrodes (gap 3.5–4 mm, depending on primary tumor size).

The summary of target pulsing protocols is shown in Table I. The typical waveform (*in vivo,* nsPEF4) is shown in Fig. 1. It can be seen that the peak voltage of the pulses was 1200 V corresponding to 3.4 kV/cm electric field (estimated as V/d, where V – measured voltage, d – gap between electrodes). The difference in the resultant PEF amplitude is less than 5% when compared to the target parameters (Table I). The protocols were also compared energy-wise (estimated by multiplying of the amplitudes of the current and voltage measurements, pulse duration and the number of pulses) for confirmation that the thermal effects can be neglected [28].

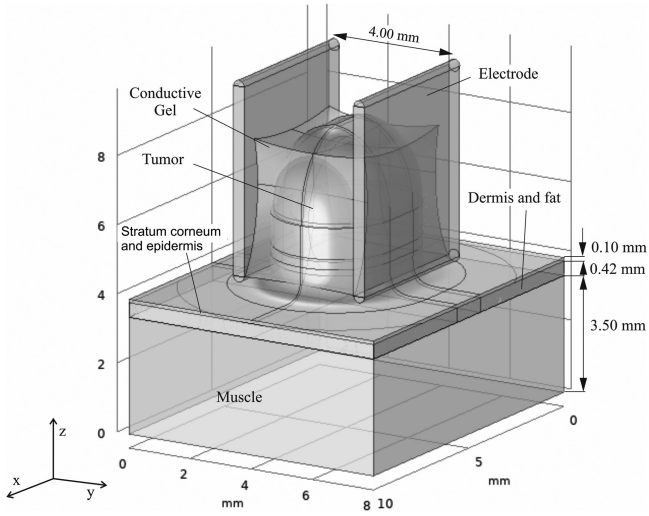

Fig. 2. FEM model of the superficial tumor positioned between two parallel plate electrodes.

TABLE II
MODEL PARAMETERS

Tissue	Thickness / Volume	Initial σ	σ increase µsPEF	σ increase nsPEF	E1/E2, kV/cm
Stratum corneum and epidermis	0.1 mm	0.03 S/m	1000	800	0.4 / 1.2
Dermis and fat	0.42 mm	0.4 S/m	6	4	0.3 / 1.2
Tumor	38 mm^3	0.5 S/m	4	2.5	0.4 / 0.8
Muscle	3.5 mm	0.5 S/m	2.5	2.5	0.15 / 0.8
Conductive gel	-	1.1 S/m	-	-	-

E1 is the threshold electric field at which the conductivity starts increasing and E2 is the electric field amplitude at which the conductivity stops increasing.

B. Finite Element Method Analysis

The three-dimensional superficial mice tumor model with non-invasive plate electrodes was introduced in this work (Fig. 2). The model involves inhomogeneity of tissue structure considering skin layers such as stratum corneum, epidermis, dermis, fat, muscle and subcutaneous tumor. Due to complexity of the skin structure and lack of availability of electrical parameters of the all the skin layers, some layers were combined and approximated as one: i.e., stratum corneum was combined with epidermis, dermis was combined with fat.

Tumor was located on mice back, therefore corresponding tissue layer thicknesses [29], [30] were introduced and summarized in Table II. The initial parameters of the model have been selected based on previous studies [31], [32] and adjusted to

match the current and voltage measurements from *in vivo* data. Conductive gel was also introduced for accurate approximation of experimental conditions.

The boundary conditions were selected using Dirichlet's and Neumann boundary conditions, where one of the electrodes stands as ground with zero potential and the second electrode transfers the applied voltage amplitude value, outer boundaries were electrically insulated. Stationary analysis has been performed. The numerical calculations were performed using COMSOL Multiphysics, version 5.5 (COMSOL, Los Angeles, CA, USA), based on finite element method.

Tissue conductivity σ cannot be treated as a constant value with one exception, when the applied voltage is sufficiently low and does not exceeds the threshold of electroporation [31]. In this experiment we apply high voltage that requires the dynamics of tissue conductivity to be considered. Therefore, for more precise calculation we include conductivity step function (smoothed Heaviside function) from initial up to the threshold value for separate multilayers i.e., stratum corneum and epidermis, dermis and fat, tumor layer and the muscle [31].

C. Luciferase Expressing LLC Carcinoma Cells

LLC1 carcinoma cells were maintained in RPMI 1640 supplemented with 2 mM glutamine, 100 U/mL penicillin, 100 mg/mL streptomycin and 10% of fetal calf serum (FCS). All cell culture reagents were obtained from Gibco (Thermo Fisher Scientific, Grand Island, NY, USA). The cells were cultured at 37 °C, 5% CO_2. LLC1 cells were electro-transfected (1.2 kV/cm $\times$ 100 μs $\times$ 4 in RMPMI medium without serum) with 0.2 μg/μl Luciferase-pcDNA3 plasmid (Adgene plasmid #18964, a kind gift from William Kaelin, Harvard Medical School, Boston, MA, USA)) [43] linearized with Bgl II. The transfected cells were selected with 200 μg/mL of G418 Sulphate (Carl Roth GmbH, Karlsruhe, Germany) and the surviving cells were cloned in 96-well plates by limiting dilution. Cells from the wells with single growing clones were tested for expression of luciferase using an *in vitro* bioluminescent assay. Half of the cells were transferred to white plates with 96 wells. D-Luciferin (Promega, Madison, WI, USA) was added to the cells to a final concentration of 150 μg/mL. The luminescence of LLC1 cells was evaluated using a Synergy 2 microplate reader and Gen5 software (BioTek, Winooski, VT, USA). The total luminescence was measured every 10 min for 6 h, at 37 °C. The cell clones were compared and selected according to the maximal luminescence (in relative light units (RLU)) over all kinetic read. Luciferase-expressing cells were grown up, frozen in medium containing 90% of fetal calf serum (FCS) and 10% of DMSO and stored in liquid nitrogen until used. The established luciferase- expressing cell lines were named LLC1-Luc.

D. Cell Permeabilization Detection Assay

Cell permeabilization was detected by flow cytometry using YO-PRO-1 (YP, Sigma-Aldrich). The 45 μl of cells in electroporation buffer (2 x 10^6 cells/ml, 242 mM saccharose, 5.5 mM Na2HPO4, 3 mM NaHPO4, 1.7 mM $MgCl_2$, pH 7.1) were mixed with YP (5 μl) for the final YP concentration of 1 μM. Out of the resulting volume the 45 μl samples were placed between the electrodes and treated by PEF followed by 10 min incubation at room temperature. Afterwards, the samples were analyzed by flow cytometry (10000 cells) using Amnis FlowSight Imaging Flow Cytometer (Luminex Corporation, Texas, USA).

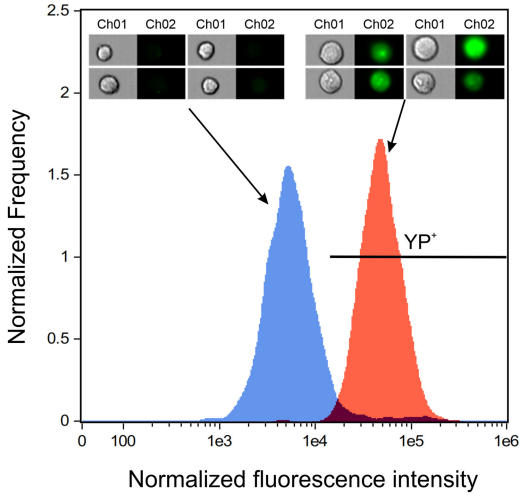

Fig. 3. Gate definition based on fluorescence spectra of treated and untreated cells, where Ch01 – brightfield images of cells; Ch02 – fluorescence image of respective cells at wavelength of 488 nm.

A shift of fluorescence spectra and the cells in the defined gate was interpreted as fluorescence positive (permeabilized), while the cells outside the gate have been interpreted as non-fluorescent (non-permeabilized). The gate was defined as shown in Fig. 3 (upper part).

The adequacy of gate definition was also confirmed by fluorescent images of cells (Fig. 3).

E. Tumor Induction and Mice Electrochemotherapy

C57BL/6 mice were bred and housed in the mouse facility of the State Research Institute Centre for Innovative Medicine (Vilnius, Lithuania). 1 $\times$ 10^6 of LLC1-Luc carcinoma cells in phosphate-buffered saline (PBS) were inoculated under the skin on the back of about 8-week-old mice. The tumors were allowed to establish and grown until they reached 5–8 mm in diameter and were then treated. Before electroporation 50 μL of bleomycin (Medac GmbH, Germany, Wedel) was injected (1500 IU, 1 mg in 50 μL) into the tumor via a single injection.

The efficiency of electroporation was evaluated by the change in tumor volumes, measured by digital caliper every 2 days. Tumor volume (mm^3) was calculated according the formula: $V = \pi lw^2/6$, where l—length and w—width of the tumor.

The mice with tumors were sacrificed when the primary tumor volumes reached more than 2000 mm^3 on the day of analysis. All experimental protocols were approved by the Lithuanian State Food and Veterinary Service (2020-04-14, No G2-145) and the study was carried out in strict accordance with the recommendations in the Guide for the Care and Use of Laboratory Animals.

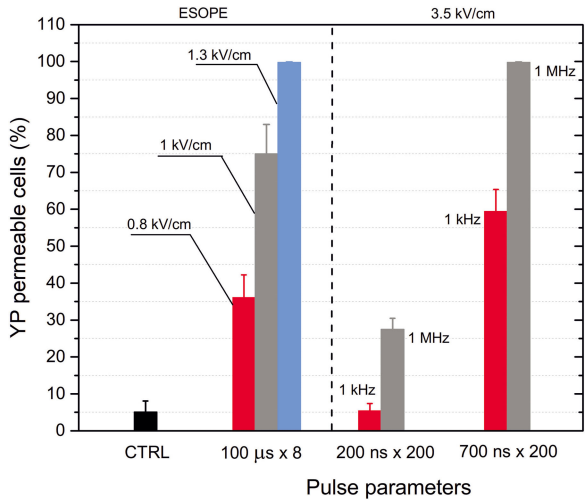

Fig. 4. Effects of pulsed electric field on membrane permeability to YP, where CTRL – untreated control.

F. Statistical Analysis

Tumor volume analysis was performed using GraphPad Prism 6 software (GraphPad Software Inc., La Jolla, San Jose, CA, USA). A nonparametric Mann-Whitney U test was used to compare tumor volumes from two groups of mice. Differences with a p-value <0.05 were regarded as significant.

III. Results

A. Electroporation In Vitro

Considering various sensitivity of cancers to PEF, firstly, the effects of PEF have been tested *in vitro* to ensure saturated permeabilization of the LLC1 cell line (i.e., further increase of treatment intensity does not result in increase of permeabilized cells). The cells have been subjected to various PEF protocols and the permeability of the cell membrane to YP has been evaluated and is shown in Fig. 4. It can be seen that 0.8 and 1 kV/cm ESOPE protocols do not trigger saturated permeabilization, thus the 1.3 kV/cm x 100 μs x 8 protocol was selected for *in vivo*. For treatment efficacy comparison purposes, it is more appropriate to use a protocol with saturated permeabilization to prevent negative-bias. The nano-range protocols, as expected, depending on the time delay between the pulses (the pulse delivery frequency was controlled) triggered different permeabilization rates. Higher energy bursts (700 ns sequences) showed better results of 60% and 100% permeabilization rate of the cells for 1 kHz and 1 MHz frequencies, respectively. The 200 ns bursts were less effective barely exceeding 25% YP-permeable cells after 1 MHz burst. The 1 kHz burst did not result in any statistically significant difference in signal versus untreated control.

B. Electrochemotherapy

All five protocols have been employed *in vivo* with bleomycin, followed by volumetric measurement of tumors for several weeks.

As can be seen (Fig. 5), the mice in the untreated control group had to be sacrificed already after only 2 weeks due to rapid tumor growth. The weakest PEF protocol (nsPEF1) elicited a definitive ($P<0.05$) reduction in tumor growth, but at best could only delay tumor development for 2-3 days. Nonetheless, the effects of the time delay between the pulses were of greatest interest, as it was possible to alter treatment efficiency without altering burst energy. As can be seen in Fig. 5, the phenomena present *in vitro* also occur *in vivo*. Basically, the triggered antitumoral response is comparable ($P>0.05$) with the ESOPE protocol. The 700 ns protocols were the most efficient since the average of the tumor volume was the lowest, however, the difference was not statistically significant. The response rates *in vivo* are in very good agreement with the results acquired *in vitro*. Nevertheless, only 3 out of 16 mice from the nsPEF3 and nsPEF4 groups were tumor-free after 4 weeks. In all the other groups the tumors started to regrow, including ESOPE.

For better understanding the reason behind the result, FEM simulation of the treatment was performed.

C. FEM Analysis

A multilayered structure of the skin, tumor and the electrodes have been simulated in COMSOL Multiphysics (COMSOL, Stockholm, Sweden) environment and the homogeneity of the applied electric field was evaluated. The results are summarized in Fig. 6.

It can be seen that the superficial tumor is squeezed up to 3.5 – 4 mm to ensure high contact area and a good exposure of the tumor. However, due to shape of the formed "lump", it's difficult to ensure contact at the top of the tumor. Similar situation is observed everywhere where the tumor surface forms a curve in respect to the parallel plate electrodes and no longer a contact can be ensured. Also, since non-invasive electrodes are employed, some inhomogeneity is observed at the bottom of the tumor too. Both these factors resulted in a treatment when the part of the tumor is affected by sub-threshold electric field. The quantitative evaluation of the fraction of the tumor volume affected by the PEF is presented in Fig. 7.

It can be seen that due to limited contact ("lump" is formed) the amplitude of the PEF within the tumor may vary more than 30%. One of the solutions is to further increase the PEF amplitude and trigger partial direct ablation of tissue. As a result, the inhomogeneity of PEF will be the same, but a higher fraction of the tumor will be subjected to above-threshold PEF required for successful electroporation. Another approach could be application of larger amount of conductive gel in order to fully sub-merge the tumor from all the sides with a significant reserve. It can be seen from Fig. 6 that this approach is effective. Nevertheless, in such a case if the gel conductivity is not selected properly there is a possibility to shunt the tumor electrically, thus negatively impacting the spatial electric field distribution inside the tumor and cause overcurrent resulting in potential generator damage.

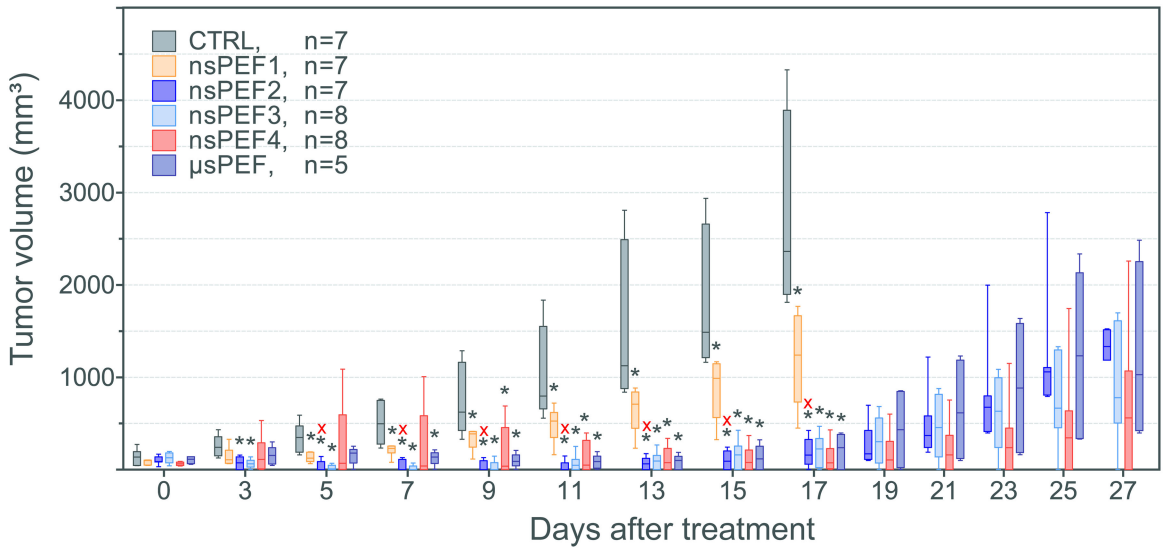

Fig. 5. Volumetric changes of the tumors after bleomycin electrochemotherapy, where nsPEF1 – 3.5 kV/cm x 200 ns x 200, 1 kHz protocol; nsPEF2 – 3.5 kV/cm x 200 ns x 200, 1 MHz protocol; nsPEF3 – 3.5 kV/cm x 700 ns x 200, 1 kHz protocol; nsPEF4 – 3.5 kV/cm x 700 ns x 200, 1 MHz; μsPEF – 1.3 kV/cm x 100 μs x 8, 1 Hz protocol; CTRL – untreated control. Asterisk ($*$) indicates statistically significant ($P<0.05$, Mann-Whitney U test) difference versus CTRL; (X) - indicates statistically significant ($P<0.05$) difference versus nsPEF1. Whiskers extend to maximum or minimum data values from the median of the dataset, while top of the boxes indicate the upper quartile, the bottom of the boxes indicate the lower quartile.

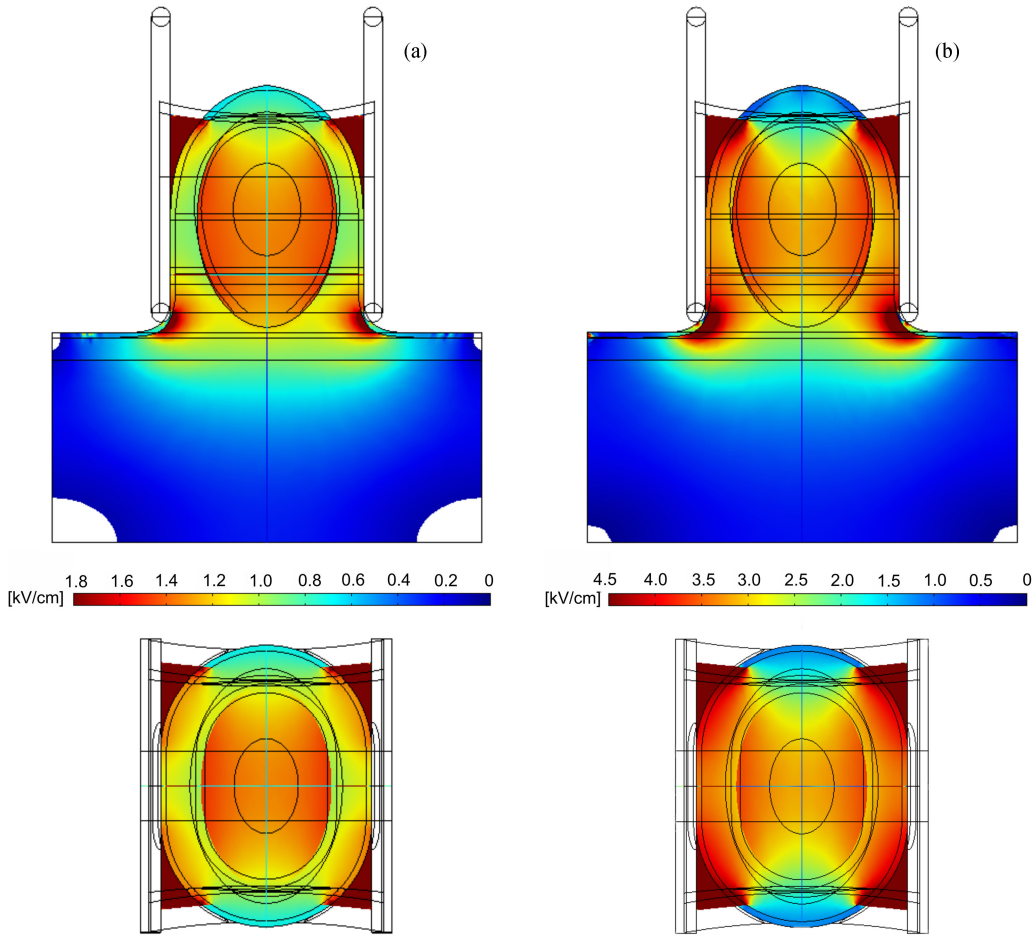

Fig. 6. The spatial distribution (x and y axis) of electric field during electrochemotherapy, where (A) 1.3 kV/cm 100 μs protocol I; (B) 3.5 kV/cm nanosecond protocol.

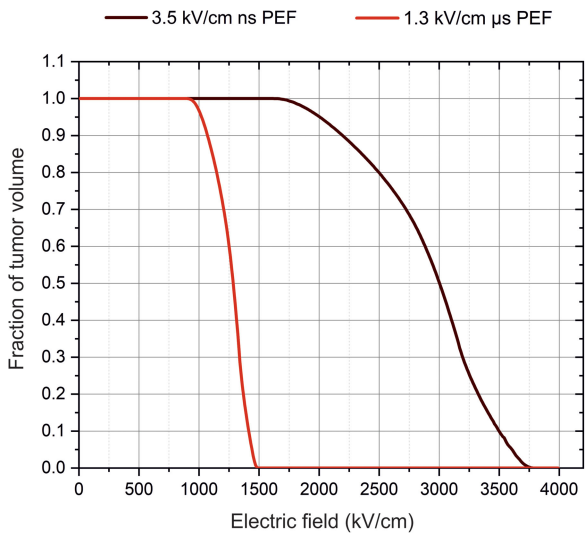

Fig. 7. Fraction of volume of tumor affected by pulsed electric field due to field non-homogeneity.

IV. Discussion

In this work we have compared the efficacy of conventional clinically used (ESOPE) protocol with a new modality of nano-electrochemotherapy, which employs ns unipolar pulse sequences for manipulation of the transmembrane voltage without alteration of the input energy (i.e., nsPEF1 versus nsPEF2).

Previously, the phenomenon of TMP accumulation during high frequency unipolar bursts was confirmed *in vitro* [22], [33] and *in silico* [34], [35]. However, in this work we have successfully confirmed the phenomenon *in vivo*. The results are in excellent agreement with *in vitro* data indicating higher permeabilization during high frequency bursts. In some sources the effect is called "MHz pulse compression" [33] and in our work the effect was particularly obvious for the 200 ns pulses, where the delivery frequency (1 MHz) dramatically potentiated the efficacy of bleomycin electrochemotherapy. The result is also in good agreement with our previous hypothesis that the phenomenon of rapid membrane charge accumulation is non-present at low repetition frequency electroporation (1 kHz) due to the delay between the pulses being longer than the relaxation time.

In this study, the electrochemotherapy efficacy was comparable between nanosecond and ESOPE pulses even though the protocols are dramatically different parameter-wise. The result has confirmed the assumption that nano-electrochemotherapy can be as effective as the ESOPE procedure, however, the nature of the saturated efficacy was not well understood at first and required FEM simulation. It was shown that the reason is the electric field non-homogeneity inside the tumor, which is due the form-factor of the tumor and limited contact area with the parallel plate electrodes. Partly the problem can be minimized by use of high amount of conductive gel and sub-merging the whole tumor in a conductive medium, however, the solution will inevitably influence the current drawn from the generator. High voltage pulses with currents exceeding 50 A and several kV in voltage form a significant technological challenge to generate when pulse repetition frequencies exceeding 1 MHz are required. Nevertheless, high frequency pulse technologies are still desirable since potentially allow to overcome the impedance barriers due to low conductivity tissues and thus, ensure a more uniform treatment. In this study, the frequency was still too low to observe significant changes in tissue bioimpedance – the current was scaling proportionally to the charged voltage in all the applied protocols. Zhao *et al.*, have reported different values for starting conductivity between 100 μs and 2 μs pulses. However, in their case, the shorter pulses were all bipolar, which resulted in a higher frequency component. In contrast, our nanosecond pulses were monopolar, which means, that the low frequency component was not canceled out over the entire pulse train duration [36]. Nevertheless, application of high frequency bursts was beneficial in terms of muscle contractions (i.e., muscle contractions induced by 200 ns were significantly lower compared to 700 ns or 100 μs procedures). ESOPE required 8 seconds for the treatment and thus induced eight separate contractions. Also, due to the higher amplitudes of PEF in nsPEF protocols, the whole treatment volume was subjected to significantly higher electric field when compared to ESOPE. It explains the reason behind the fully recovered mice being present only in nsPEF groups.

V. Conclusion

To conclude, the delay between nanosecond pulses plays a dramatic role on the outcome of electrochemotherapy. The efficacy of tumor inhibition can be effectively manipulated solely by the pulse delivery frequency without changing of the input energy.

Acknowledgment

The authors declare no conflict of interest. The funders had no role in the design of the study, in the collection, analyses or interpretation of data; in the writing of the manuscript, or in the decision to publish the results.

References

[1] D. Shamoon *et al.*, "Assessing the electro-deformation and electroporation of biological cells using a three-dimensional finite element model," *Appl. Phys. Lett.*, vol. 14, no. 6, 2019, Art. no. 063701.

[2] T. García-Sánchez, C. Merla, J. Fontaine, A. Muscat, and L. M. Mir, "Sine wave electropermeabilization reveals the frequency-dependent response of the biological membranes," *Biochim. Biophys. Acta Biomembr.*, vol. 1860, no. 5, pp. 1022–1034, Feb. 2018.

[3] G. Pucihar, J. Krmelj, M. Reberšek, T. B. Napotnik, and D. Miklavčič, "Equivalent pulse parameters for electroporation," *IEEE Trans. Biomed. Eng.*, vol. 58, no. 11, pp. 3279–3288, Nov. 2011.

[4] S. Romeo *et al.*, "ESOPE-equivalent pulsing protocols for calcium electroporation: An in vitro optimization study on 2 cancer cell models," *Technol. Cancer Res. Treat.*, vol. 14, 2018, Art. no. 153303381878807.

[5] E. C. Gianulis, C. Labib, G. Saulis, V. Novickij, O. N. Pakhomova, and A. G. Pakhomov, "Selective susceptibility to nanosecond pulsed electric field (nsPEF) across different human cell types," *Cell. Mol. Life Sci.*, vol. 74, pp. 1741–1754, 2016.

[6] E. Pirc, D. Miklavcic, and M. Rebersek, "Nanosecond pulse electroporator with silicon carbide MOSFETs, development and evaluation," *IEEE Trans. Biomed. Eng.*, vol. 66, no. 12, pp. 3526–3533, Dec. 2019.

[7] I. W. Davies and C. P. Hancock, "An ultrashort electric field pulse generator using avalanche breakdown transistors and the open circuit transmission line technique for nanosecond electroporation," in *Asia-Pacific Microw. Conf. Proc.*, 2019, pp. 1289–1291.

[8] B. Rubinsky, G. Onik, and P. Mikus, "Irreversible electroporation: A new ablation modality - Clinical implications," *Technol. Cancer Res. Treat.*, vol. 6, pp. 37–48, 2007.

[9] R. V. Davalos and B. Rubinsky, "Temperature considerations during irreversible electroporation," *Int. J. Heat Mass Transf.*, vol. 51, pp. 5617–5622, 2008.

[10] C. Jiang, R. V. Davalos, and J. C. Bischof, "A review of basic to clinical studies of irreversible electroporation therapy," *IEEE Trans. Biomed. Eng.*, vol. 62, no. 1, pp. 4–20, Jan. 2015.

[11] R. V. Davalos, L. M. Mir, and B. Rubinsky, "Tissue ablation with irreversible electroporation," *Ann. Biomed. Eng.*, vol. 33, pp. 223–231, 2005.

[12] D. Miklavčič, B. Mali, B. Kos, R. Heller, and G. Serša, "Electrochemotherapy: From the drawing board into medical practice.," *Biomed. Eng. Online*, vol. 13, no. 1, pp. 29, 2014.

[13] M. Marty *et al.*, "Electrochemotherapy - An easy, highly effective and safe treatment of cutaneous and subcutaneous metastases: Results of ESOPE (European standard operating procedures of electrochemotherapy) study," *Eur. J. Cancer, Suppl.*, vol. 4, no. 11, pp. 3–13, 2006.

[14] R. Sundararajan, "Nanosecond electroporation: Another look," *Mol. Biotechnol.*, vol. 41, no. 1, pp. 69–82, 2009.

[15] A. G. Pakhomov, E. Gianulis, P. T. Vernier, I. Semenov, S. Xiao, and O. N. Pakhomova, "Multiple nanosecond electric pulses increase the number but not the size of long-lived nanopores in the cell membrane," *Biochim. Biophys. Acta Biomembr.*, vol. 1848, no. 4, pp. 958–966, 2015.

[16] K. H. Schoenbach, B. Y. Hargrave, R. P. Joshi, J. F. Kolb, and R. Nuccitelli, "Bioelectric effects of intense ultrashort pulses.," *Crit. Rev. Biomed. Eng.*, vol. 38, no. 3, pp. 255–304, 2010.

[17] R. Nuccitelli, K. Tran, S. Sheikh, B. Athos, M. Kreis, and P. Nuccitelli, "Optimized nanosecond pulsed electric field therapy can cause murine malignant melanomas to self-destruct with a single treatment," *Int. J. Cancer*, vol. 127, pp. 1727–1736, 2010.

[18] J. Tunikowska, A. Antończyk, N. Rembiałkowska, Ł. Jóźwiak, V. Novickij, and J. Kulbacka, "The first application of nanoelectrochemotherapy in feline oral malignant melanoma treatment— Case study," *Animals*, vol. 10, p. 556, 2020.

[19] Z. Łapińska, M. Dębiński, A. Szewczyk, A. Choromańska, J. Kulbacka, and J. Saczko, "Electrochemotherapy with calcium chloride and 17β-estradiol modulated viability and apoptosis pathway in human ovarian cancer," *Pharmaceutics*, vol. 13, pp. 1–17, 2021.

[20] V. Novickij *et al.*, "Electrochemotherapy using doxorubicin and nanosecond electric field pulses: A pilot in vivo study," *Molecules*, vol. 25, no. 20, pp. 1–12, 2020.

[21] A. Vižintin, S. Marković, J. Ščančar, and D. Miklavčič, "Electroporation with nanosecond pulses and bleomycin or cisplatin results in efficient cell kill and low metal release from electrodes," *Bioelectrochemistry*, vol. 140, Aug. 2021, Art. no. 107798.

[22] V. Novickij, P. Ruzgys, A. Grainys, and S. Šatkauskas, "High frequency electroporation efficiency is under control of membrane capacitive charging and voltage potential relaxation," *Bioelectrochemistry*, vol. 119, pp. 92–97, 2018.

[23] I. Semenov, M. Casciola, B. L. Ibey, S. Xiao, and A. G. Pakhomov, "Electropermeabilization of cells by closely spaced paired nanosecond-range pulses," *Bioelectrochemistry*, vol. 121, pp. 135–141, 2018.

[24] Y. Mi, J. Xu, C. Yao, C. Li, and H. Liu, "Electroporation modeling of a single cell exposed to high-frequency nanosecond pulse bursts," *IEEE Trans. Dielectr. Electr. Insul.*, vol. 26, no. 2, pp. 461–468, Apr. 2019.

[25] A. Murauskas *et al.*, "Predicting electrotransfer in ultra-high frequency sub-microsecond square wave electric fields," *Electromagn. Biol. Med.*, vol. 39, pp. 1–8, 2020.

[26] T. Polajžer, J. Dermol-Černe, M. Reberšek, R. O'Connor, and D. Miklavčič, "Cancellation effect is present in high-frequency reversible and irreversible electroporation," *Bioelectrochemistry*, vol. 132, 2020, Art. no. 107442.

[27] V. Novickij *et al.*, "High-frequency submicrosecond electroporator," *Biotechnol. Biotechnol. Equip.*, vol. 30, no. 3, pp. 607–613, May 2016.

[28] R. Nuccitelli *et al.*, "Nanosecond pulsed electric fields cause melanomas to self-destruct," *Biochem. Biophys. Res. Commun.*, vol. 343, pp. 351–360, 2006.

[29] J. C. J. Wei, G. A. Edwards, D. J. Martin, H. Huang, M. L. Crichton, and M. A. F. Kendall, "Allometric scaling of skin thickness, elasticity, viscoelasticity to mass for micro-medical device translation: From mice, rats, rabbits, pigs to humans," *Sci. Rep.*, vol. 7, 2017, Art. no. 15885.

[30] J. Hew *et al.*, "The effects of dietary macronutrient balance on skin structure in aging male and female mice," *PLoS One*, vol. 11, 2016, Art. no. e0166175.

[31] S. Corovic, I. Lackovic, P. Sustaric, T. Sustar, T. Rodic, and D. Miklavcic, "Modeling of electric field distribution in tissues during electroporation," *Biomed. Eng. Online*, vol. 12, pp. 1–27, 2013.

[32] N. Pavšelj and D. Miklavčič, "Numerical models of skin electropermeabilization taking into account conductivity changes and the presence of local transport regions," *IEEE Trans. Plasma Sci.*, vol. 36, no. 4, pp. 1650–1658, Aug. 2008.

[33] A. G. Pakhomov *et al.*, "Excitation and electroporation by MHz bursts of nanosecond stimuli," *Biochem. Biophys. Res. Commun.*, vol. 518, pp. 759–764, 2019.

[34] Y. Mi, J. Xu, X. Tang, C. Yao, and C. Li, "Electroporation simulation of a multicellular system exposed to high-frequency 500 ns pulsed electric fields," *IEEE Trans. Dielectr. Electr. Insul.*, vol. 24, no. 6, pp. 3985–3994, Dec. 2017.

[35] F. Guo, K. Qian, L. Zhang, X. Liu, and H. Peng, "Multiphysics modelling of electroporation under uni- or bipolar nanosecond pulse sequences," *Bioelectrochemistry*, vol. 141, 2021, Art. no. 107878.

[36] Y. Zhao *et al.*, "Characterization of conductivity changes during high-frequency irreversible electroporation for treatment planning," *IEEE Trans. Biomed. Eng.*, vol. 65, no. 8, pp. 1810–1819, Aug. 2018.